Deconstructing complex Au-Ag-Cu mineralization, Sonora Gulch project, Dawson Range: A Late Cretaceous evolution to the epithermal environment

Venessa Bennett[1]
Yukon Geological Survey

Carl Schulze[2]
All-Terrane Mineral Exploration Services

Dennis Ouellette[3] ***and Bonnie Pollries***[4]
Northern Tiger Resources

Bennett, V., Schulze, C., Ouellette, D. and Pollries, B., 2010. Deconstructing complex Au-Ag-Cu mineralization, Sonora Gulch project, Dawson Range: A Late Cretaceous evolution to the epithermal environment. *In*: Yukon Exploration and Geology 2009, K.E. MacFarlane, L.H. Weston and L.R. Blackburn (eds.), Yukon Geological Survey, p. 23-45.

ABSTRACT

We present new field and U-Pb analytical data from the Sonora Gulch Project that demonstrate a protracted history of polymetallic mineralization (Au-Ag-Cu-Zn ± Mo) associated with several pulses of Cretaceous magmatism. Recent exploration on the Sonora Gulch Project has highlighted the presence of two important mineralized zones: the Nightmusic zone, a mesothermal Au-enriched base metal skarn, and the Amadeus zone, an epithermal Au-Ag system. Four U-Pb age dates determined from each of two feldspar porphyry dykes (ca. 74 Ma), a weakly mineralized quartz porphyry stock (ca. 75 Ma) within the Nightmusic zone and the Au-Ag mineralized Amadeus stock (ca. 75 Ma), demonstrate the widespread occurrence of Late Cretaceous magmatism. The age determinations indicate that mineralization occurring within the Sonora Gulch project area are temporally equivalent to the Casino Cu-Au-Mo deposit, located roughly 40 km to the west-northwest. These new data extend the currently known eastern limit of Late Cretaceous magmatism and associated mineralization.

[1]*venessa.bennett@gov.yk.ca*

[2]*allterrane@northwestel.net*

[3]*douellette@firestoneventures.com*

[4]*bpollries@northern-tiger.com*

INTRODUCTION

The Sonora Gulch property, which is wholly owned by Northern Tiger Resources Inc., is located in the central Dawson Range, west-central Yukon where it forms part of a regionally extensive, northwest-trending polymetallic mineral belt associated with Early Jurassic (*e.g.*, Minto deposit) to latest Cretaceous magmatism (*e.g.*, Casino deposit; Figs. 1, 2). An important characteristic of metal concentration occurring throughout the belt is the superposition of mineralizing events upon pre-existing ores, such that early phase mineralization can be significantly enriched and/or remobilized along active structural corridors to be subsequently re-deposited at structurally and chemically favourable sites (*e.g.*, Mortensen *et al.*, 2002; Bineli Betsi and Bennett, this volume). Importantly, the Sonora Gulch property occurs where a major regional northwest-trending structure, the Big Creek fault, intersects both mid- and Late Cretaceous magmatism and hence represents a highly desirable location to explore for economically important concentrations of metals. Placer gold mines have operated on streams draining the Sonora Gulch property since the turn of the 20th century, recovering angular nuggets of gold, commonly with tetradymite (a bismuth telluride).

Historical exploration conducted on the property identified two main mineralized zones including: (i) a kilometre-scale zone of anomalous Cu-Au mineralization hosted by a pyritic quartz-feldspar porphyritic intrusion; and (ii) a zone of gold-tetradymite quartz vein-hosted

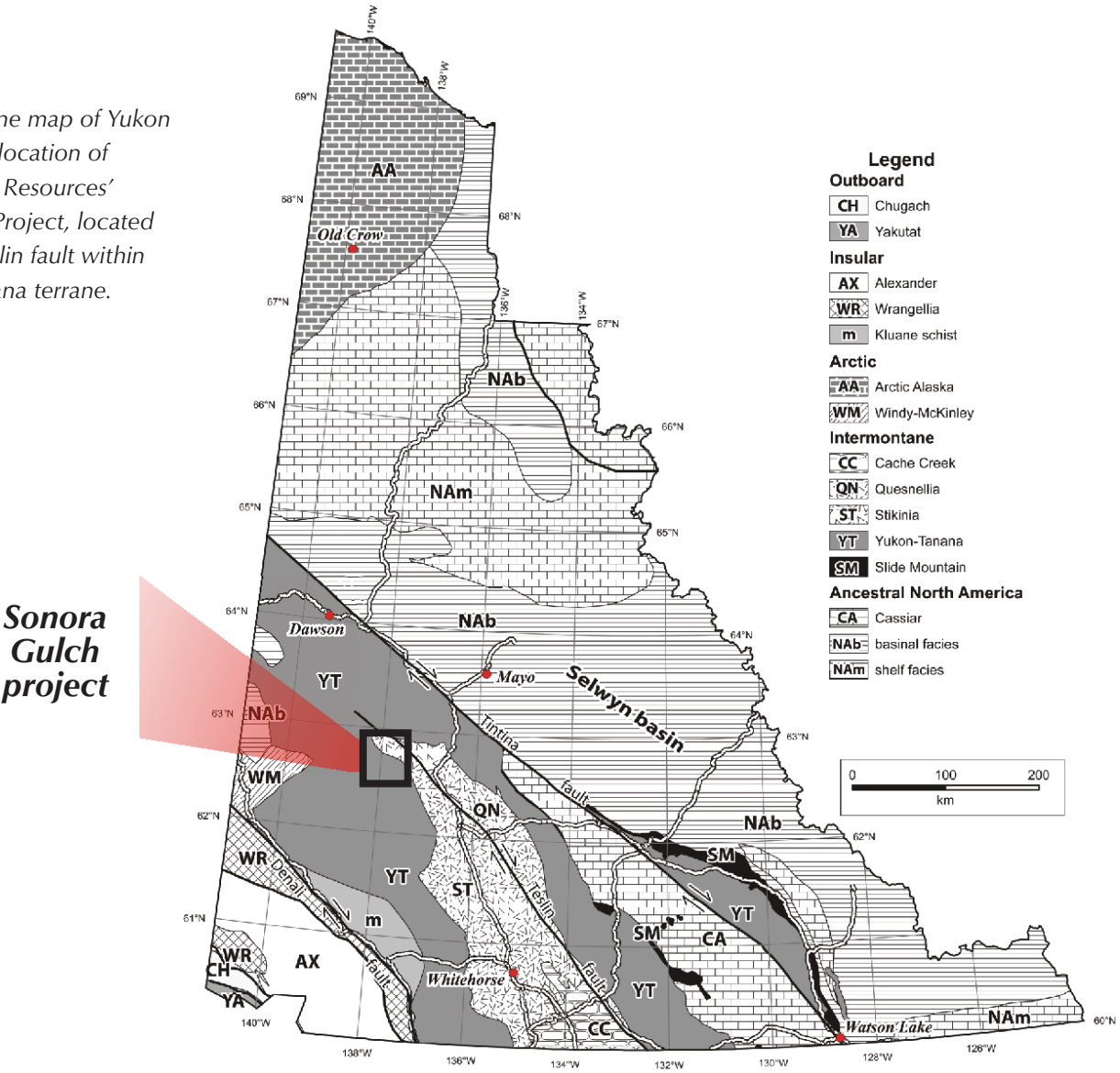

Figure 1. *Terrane map of Yukon illustrating the location of Northern Tiger Resources' Sonora Gulch Project, located west of the Teslin fault within the Yukon-Tanana terrane.*

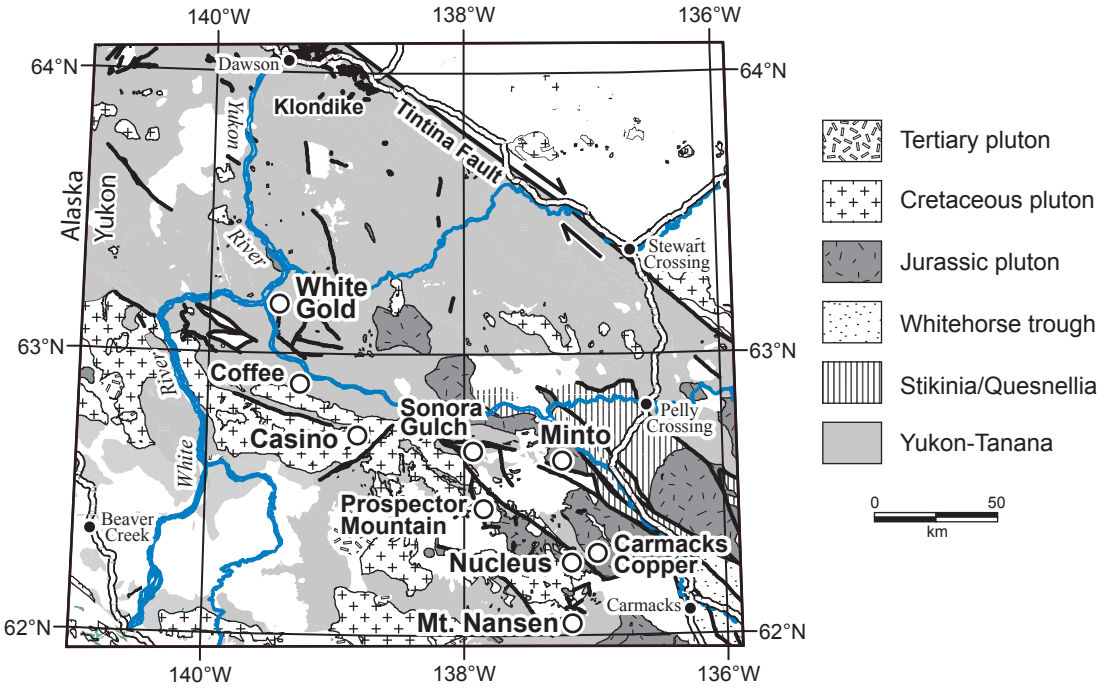

Figure 2. *Regional geological map illustrating distribution of main mineral occurrences and deposits within the Dawson Range (courtesy of M. Colpron). Location of Sonora Gulch camp marked.*

mineralization oriented northwest, approximately along the interpreted trace of the Big Creek fault. In addition to these historical zones, recent exploration on the Sonora Gulch project has highlighted the presence of several zones of important Au-Ag ± Cu ± Zn ± Mo mineralization, the most advanced being the Nightmusic (mesothermal skarn/replacement) and Amadeus zones (epithermal stock; Fig. 3; Schulze, 2004, 2007a,b). In this contribution, we present new field and U-Pb analytical data from the Nightmusic and Amadeus zones that demonstrate a protracted history of polymetallic mineralization associated with discrete pulses of Cretaceous magmatism.

DISTRICT GEOLOGY

The Sonora Gulch property lies entirely within the Yukon-Tanana terrane, an accreted terrane locally separated from strata of the ancestral North American margin by the northwest-trending Tintina fault. The Yukon-Tanana terrane consists of a belt of Late Devonian to Late Permian metamorphic rocks, including various metasedimentary and metavolcanic assemblages, and up to four distinct suites of calc-alkaline metaplutonic rocks (Mortensen, 1992; Colpron *et al.*, 2006). The northwest-trending Denali (Shakwak) fault, located approximately 140 km to the southwest, forms the southwestern boundary of the Yukon-Tanana terrane (Gordey and Makepeace, 1999; Davidson, 2000).

In the Dawson Range, the Yukon-Tanana terrane typically includes metasedimentary and metavolcanic sequences of quartz-mica schist and diorite gneiss. Plutonic rocks of the mid-Cretaceous Dawson Range batholith intrude the Yukon-Tanana terrane over vast areas and consist of large bodies of granodiorite and quartz monzonite, and smaller high-level felsic porphyry plugs and sills. Locally, narrow ultramafic units of unknown age have been emplaced along major structures within the Yukon-Tanana terrane. A suite of quartz-eye feldspar ± biotite porphyritic monzonite to granite intrusions, including felsic dykes, was previously interpreted as part of the mid-Late Cretaceous Prospector Mountain suite (Davidson, 2000). Late volcanic rocks in the district consist of sills, dykes and flows of the Late Cretaceous Mount Nansen Group, and mafic flows and pyroclastic volcanic rocks of the Late Cretaceous Carmacks Group (Templeman-Kluit, 1984, Davidson, 2000).

Two regional-scale faults crosscut the region: the northwest-trending Big Creek fault and an east-trending fault. The Big Creek fault, which extends northwest approximately 80 km from the Freegold Mountain property of Northern Freegold Resources Ltd., intersects the east fault, west of the junction of Selkirk and Hayes creeks. From this intersection, the Big Creek fault projects more westerly in orientation. Importantly, the Big Creek fault and related northwest-trending faults are considered to represent the locus of an important mineralizing belt,

extending possibly as far as the Casino deposit of Western Copper Inc. Copper porphyry and structurally hosted gold deposits occur ubiquitously along these northwest to north-northwest-trending fault systems, and associated placer gold deposits occur within watersheds draining these mineralized zones.

GEOLOGY OF SONORA GULCH PROPERTY

The Sonora Gulch property is underlain by polydeformed and metamorphosed Devonian to Mississippian metagranitic, metavolcanic and subordinate metasedimentary rocks assigned to the Wolverine Creek metamorphic suite of the Yukon Tanana terrane (Johnston and Hachey, 1993). Several ultramafic sills and numerous mid- and Late Cretaceous monzonitic – granitic magmatic units intrude the Wolverine Creek assemblage within the property area (Fig. 3). West of Hayes Creek, several

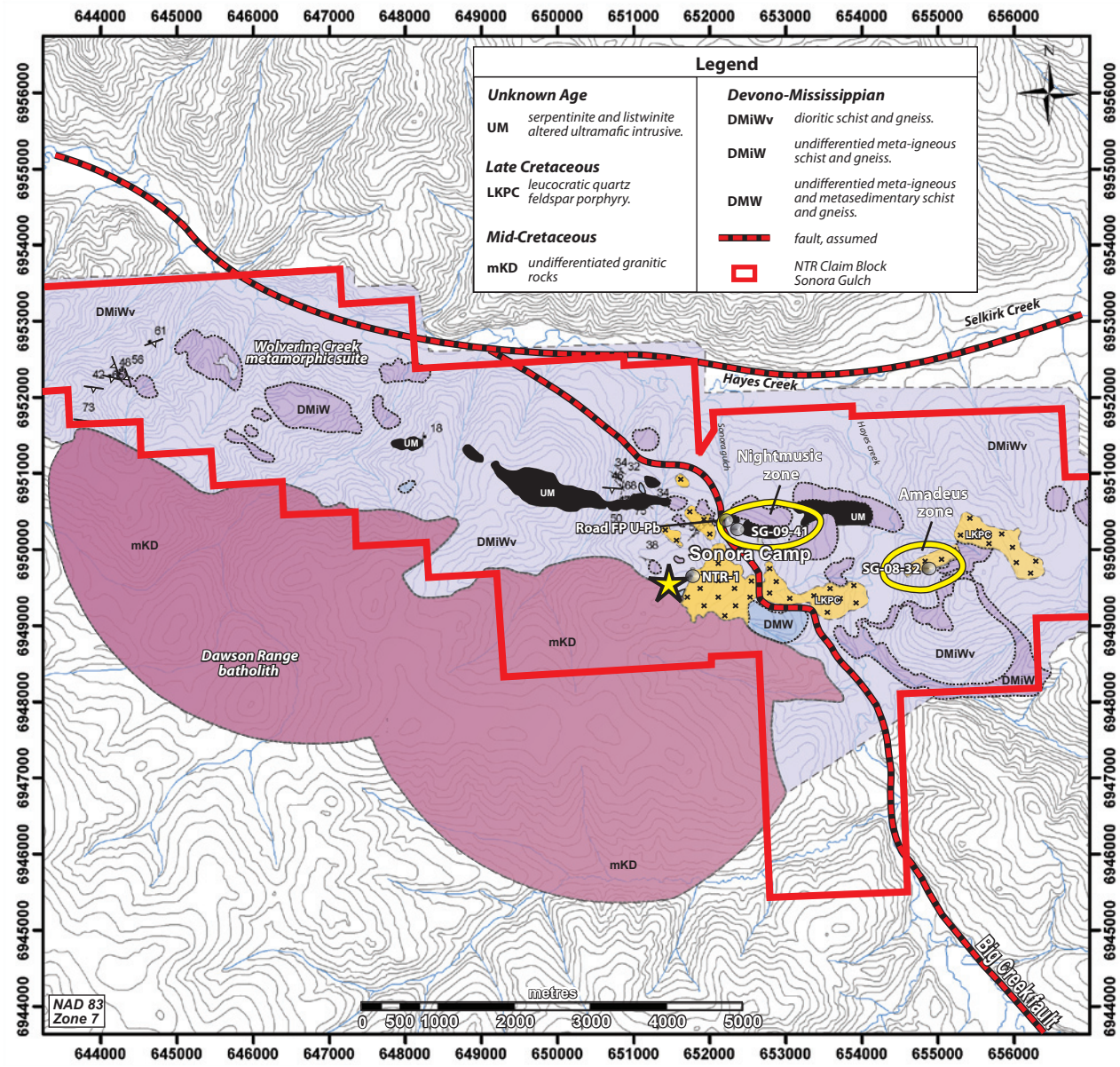

Figure 3. *Property geology map, Sonora Gulch project, 2009, Northern Tiger Resources. Location of the Nightmusic and Amadeus zones and sampling localities for U-Pb geochronology marked. Star indicates position of camp.*

ultramafic lenses are intercalated within the west-northwest striking Wolverine Creek units. Importantly, these ultramafic bodies are spatially associated with mineralization occurring in the Nightmusic zone. The mid-Cretaceous east-southeast-trending Dawson Range batholith occurs along the southwest margin of the Sonora Gulch property, west of the Big Creek fault (Fig. 3). Late Cretaceous quartz-feldspar porphyritic monzonite of the Prospector Mountain suite intrudes the Wolverine Creek sequence along the northern boundary of the Dawson Range batholith, east of the Sonora camp. Furthermore, this monzonitic stock is crosscut by the Big Creek fault (Fig. 3). East of Hayes Creek, a small stock of strongly pyritic feldspar porphyritic monzonite, called the Amadeus stock, occurs in association with significant Au-Ag mineralization.

WOLVERINE CREEK METAMORPHIC SUITE

Metabasaltic rocks represent the most aerially extensive member of the Wolverine Creek suite within the Sonora Gulch property area. They are typically strongly foliated and characterized by a well-developed gneissic fabric. Metabasaltic rocks have a weak to moderate calcareous composition and are commonly host to replacement-style and skarn mineralization within the Nightmusic zone. Granitic gneiss underlies much of the Sonora Gulch property and most commonly occurs as augen gneiss characterized by quartz and feldspar augen porphyroclasts up to 0.5 cm in length. Granitic gneiss hosts a greater proportion of foliation-parallel quartz veining than metabasalts, as well as more pervasive sericite alteration and weak pyrite mineralization. Metasedimentary rocks of the Wolverine Creek suite, which underlie most of the northeastern part of the property, consist of phyllite, siltstone and mudstone, with lesser sandstone. They are variably calcareous, and include minor limestone horizons. Metasedimentary rocks exhibit a prominent schistose foliation, with variable and locally intense sericite and/or phlogopite alteration.

ULTRAMAFIC UNITS

Discontinuous lenses and irregular bodies of a strongly serpentinized and listwanite-altered ultramafic body occur in an east-trending structural corridor immediately east and west of the Big Creek fault. Where not completely altered, the composition of the ultramafic unit is primarily pyroxenitic. Pervasive secondary carbonate-silica alteration has resulted in destructive listwanite-alteration of the body, particularly proximal to the southern hanging wall contacts. The ultramafic lens has undergone significant deflection (*ca.* 500 m) related to dextral motion along the Big Creek fault (Fig. 4). Additionally, three separate ultramafic horizons have been identified west of the Big Creek fault.

CRETACEOUS MAGMATIC UNITS

Within the Sonora Gulch property, the mid-Cretaceous Dawson Range batholith varies from quartz-hornblende-biotite granodiorite, quartz monzonite and quartz diorite to granite. Textures are typically coarse grained and equigranular. A Late Cretaceous intrusive unit, which abuts the northern contact of the Dawson Range batholith is a massive quartz-feldspar porphyritic monzonite characterized by 35 to 40% evenly distributed feldspar grains approximately 2-3 mm in length and hosted in an aphanitic groundmass. The Late Cretaceous Amadeus stock varies from 50 m to 250 m in width and is monzonitic in composition. The stock is strongly leached and has undergone moderate to strong argillic and moderate phyllic alteration that largely masks primary textures.

MINERALIZATION

Two zones of historical mineralization occur on the Sonora Gulch property: a kilometre-scale zone of anomalous copper-gold mineralization, called the 'Gold Vein System', located towards the western end of a Late Cretaceous quartz-feldspar porphyritic monzonite stock; and a gold-tetradymite vein system, known as the 'Tetradymite Vein System', occurring several hundred metres to the north of the 'Gold Vein System' and paralleling the approximate surface trace of the Big Creek fault for approximately 1.3 km. The 'Gold Vein System' consists of disseminated pyrite and minor chalcopyrite with total sulphide concentrations approaching 10%. Gold and copper mineralization occurs both in the interior of the monzonitic stock and also along northwest-trending shear zones and fractures. Locally, the underlying unoxidized zone contains gold-bearing quartz-arsenopyrite veins with sphalerite, galena and stibnite. Precious metal content within the 'Gold Vein System' appears to be directly associated with depth, sulphide content and quartz vein density. A sample of the monzonitic stock from the 'Gold Vein System' was sampled for U-Pb age dating (sample NTR-1). Mineralization within the 'Tetradymite Vein System' is

confined to narrow, high-grade quartz-arsenopyrite veins of limited strike length.

Recent exploration on the Sonora Gulch property has defined the presence of several zones of anomalous gold including the Nightmusic and Amadeus zones, and the Sonata, Jupiter, Wolfgang and Concerto anomalies. The Nightmusic and Amadeus zones represent the most advanced of the anomalies thus far identified. The two zones are marked by distinct mineralization styles and metal suites. Mineralization in the Nightmusic zone is complex and consists of: (i) mesothermal Au-enriched base-metal skarns (Cu-Zn-Pb), (ii) replacement zones hosted by calcareous metaclastic and metavolcanic rocks, (iii) bonanza-style lode gold associated with listwanitic ultramafic rocks, and (iv) structurally controlled veins and stockwork. In contrast, the Amadeus zone represents a high-level epithermal Au-Ag mineralizing system. Importantly, the two mineralized zones occur along that portion of an east-trending structural corridor located east of the northwest-trending Big Creek fault. Farther south within the Freegold Mountain Project area, similar east-trending mineralizing structures occur to the west of the Big Creek fault, suggesting the fault system may represent a significant mineralizing conduit of regional extent.

The Nightmusic zone was initially identified through re-interpretation of historical diamond drilling results, and from a single 2007 drillhole designed to target the east-trending ultramafic horizon (Figs. 3, 4). The zone was further delineated during drill testing in 2008 and 2009. Replacement and skarn-style mineralization hosting significant gold and base-metal concentrations occur along the southern hanging wall side of the east-trending ultramafic body. Mineralized zones also occur adjacent to, or within, listwanitic ultramafic horizons, with visible gold identified at one location within the ultramafic unit. Replacement-style gold mineralization, which occurs more commonly in the western Nightmusic zone (Fig. 5a,b), appears to contain the highest grades of gold recognized thus far. In contrast, skarn mineralization and associated calc-silicate alteration that occurs at the eastern end of the Nightmusic zone hosts greater concentrations of base metals (Zn-Cu-Pb) with subordinate gold (Fig. 5e-h). The lateral variation in metal suites within the Nightmusic zone, ranging from gold-enrichment in the west to base-metal enrichment in the east, may indicate lateral zoning in a mesothermal skarn mineralizing system. The magmatic source for the Nightmusic skarn zone has yet to be located.

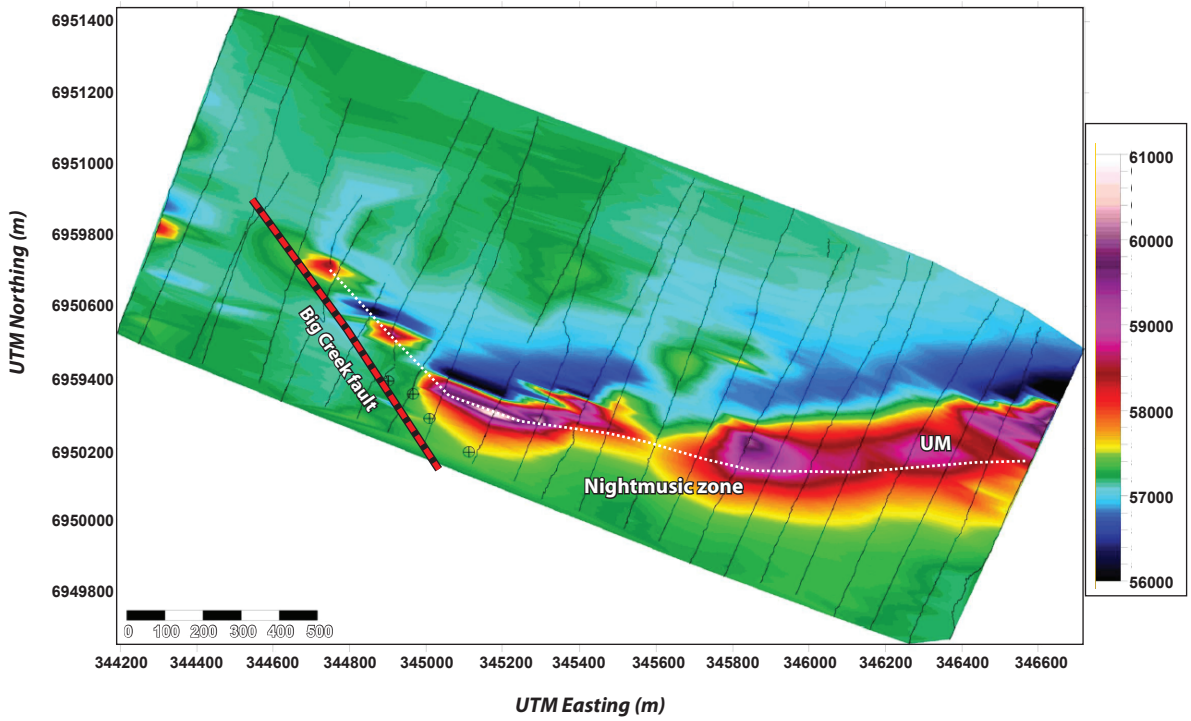

Figure 4. *Ground magnetic survey across the Nightmusic zone. The dataset highlights the location of the ultramafic unit (UM) and its deformation associated with dextral movement along the Big Creek fault. White dotted line represents the trend of the ultramafic body.*

Figure 5. *Replacement-style and skarn mineralization occurring in the Nightmusic zone;* ***(a)*** *to* ***(d)*** *replacement-style Au-Cu mineralization (DDH SG-08-27). Note:* ***(b)*** *and* ***(d)*** *show chalcopyrite (Cp) replaced by later pyrite (Py) + pyrrhotite (Po);* ***(c)*** *and* ***(d)*** *show epithermal veins crosscutting replacement-style Au mineralization. Scale bars represent 1 cm.*

Sulphide paragenesis in both replacement and skarn-style mineralized zones indicates early phase chalcopyrite ± sphalerite partially to completely overprinted by pyrite + pyrrhotite, with pyrrhotite recognized as the latest sulphide phase (Fig. 5b, e-i). Accessory molybdenite occurs in association with the Cu-Zn skarn of the eastern Nightmusic zone (Fig. 5i). Late-stage overprinting veining with epithermal textures is ubiquitous throughout the Nightmusic zone, where they are observed to crosscut both replacement and skarn mineralization (Fig. 5c,d,j).

The epithermal veins indicate the occurrence of multiple fluid and mineralizing events within the Nightmusic zone. Feldspar porphyry dykes, that are interpreted to postdate replacement and skarn mineralization, also intrude the Nightmusic zone (Fig. 6). The dykes are commonly limonite ± hematite-altered and do not host appreciable mineralization. Two feldspar porphyry dykes from the Nightmusic zone were sampled for U-Pb geochronology, one of which is crosscut by the Big Creek fault (sample SG-09-41). Brecciation and fracturing of the porphyry

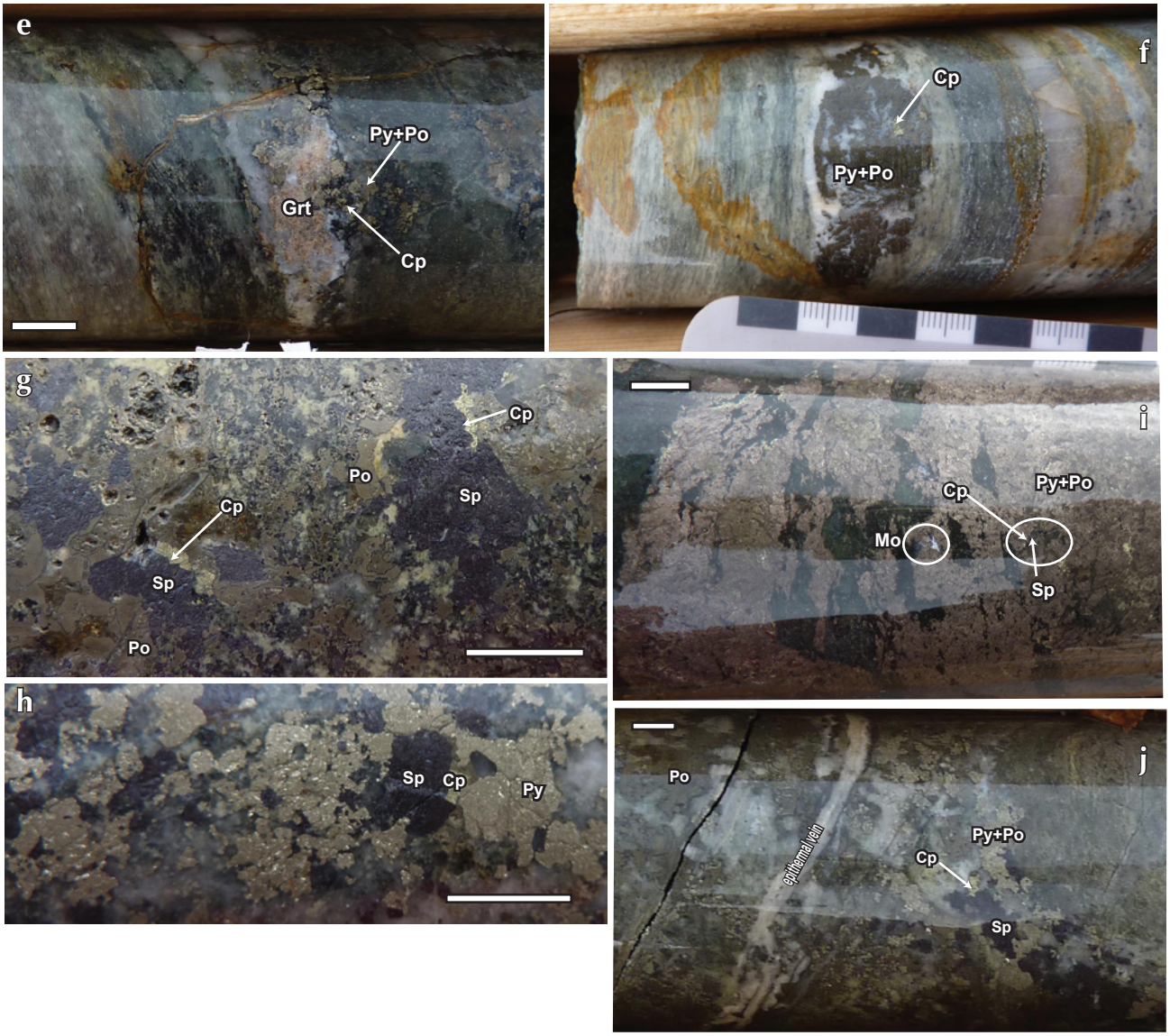

Figure 5. *continued.* ***(e)*** *Garnet + chalcopyrite replaced by pyrite + pyrrhotite in skarn zone, SG-09-43.* ***(f)*** *Sulphide vein replacement mineralization in skarn-altered gneissic host rock, Nightmusic zone, SG-09-43. Figures 5* ***(g)*** *and* ***(h)*** *sphalerite - chalcopyrite skarn mineralization overprinted by pyrite + pyrrhotite, Nightmusic zone, SG-09-43.* ***(i)*** *Sphalerite-chalcopyrite and rare molybdenite replaced by pyrite + pyrrhotite.* ***(j)*** *Late, overprinting epithermal vein crosscutting Cu-Zn skarn mineralization, SG-09-43, Nightmusic zone. Scale bars represent 1 cm. Cp = chalcopyrite, Py = pyrite, Po = pyrrhotite, Grt = garnet, Sp = Sphalerite.*

indicates that deformation and movement associated with the Big Creek fault post-dated dyke emplacement.

The Amadeus zone (Fig. 3) is hosted by a high-level, epithermal quartz-feldspar porphyritic stock, which is strongly leached and has undergone moderate to strong pervasive argillic alteration and lesser silicification. Gold and silver mineralization occurs both in the Yukon-Tanana terrane host rocks immediately above the intrusive contact of the stock and within the stock itself. Immediately above the intrusion, granitic gneiss hosts multiple phases of pyrite ± chalcopyrite vein and fracture

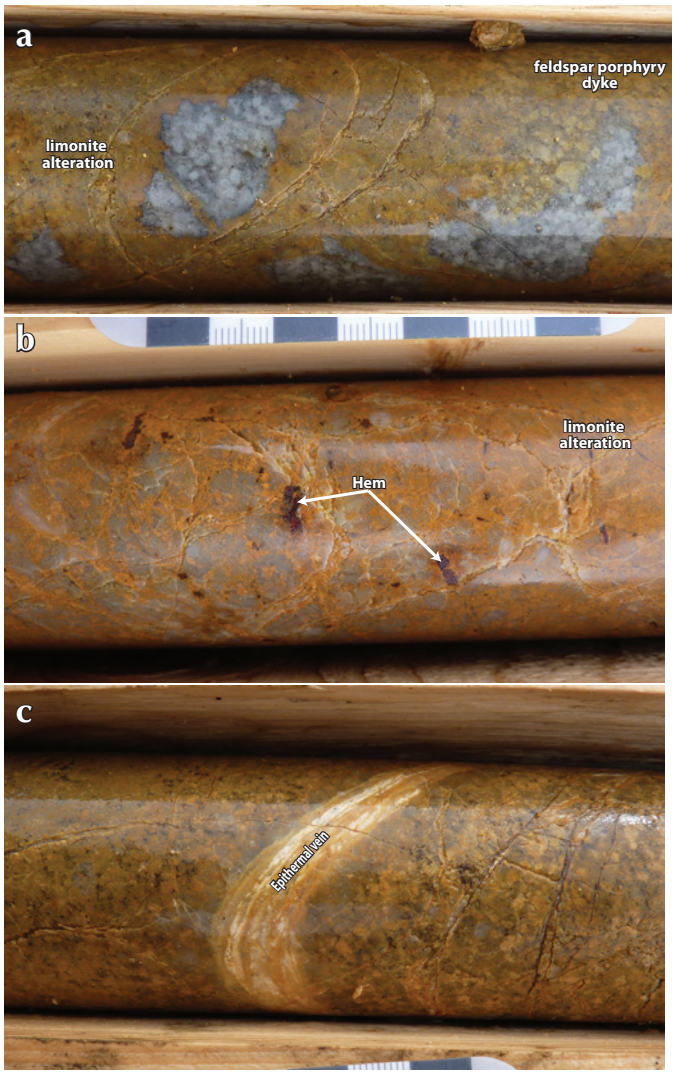

Figure 6. *Altered feldspar porphyry dykes intruding Nightmusic zone (DDH SG-09-43).* ***(a)*** *Near-complete fracture-controlled limonite alteration of feldspar porphyry dyke.* ***(b)*** *Hematite-limonite alteration of feldspar porphyry dyke.* ***(c)*** *Late-stage epithermal vein crosscutting limonite-altered feldspar porphyry dyke. Hem = hematite.*

mineralization (Fig. 7a,b). Gold and silver mineralization also occurs at the brecciated intrusive contact of the Amadeus stock and the Yukon-Tanana terrane, where pyrite ± Au and Ag mineralization occur as matrix minerals of the intrusive clast-supported breccia (Figs. 7c and 8). Within the Amadeus stock, gold and silver show a correlation with depth; gold occurs at higher levels, while appreciable silver concentrations occur at depth (Fig. 8). Gold is typically associated with fine-grained disseminated euhedral pyrite (Fig. 7d) and shows a correlation with clay alteration assemblages. Intervals of higher grade gold are typically associated with low to background arsenic values, suggesting a more evolved epithermal nature of gold mineralization. Silver mineralization within the stock is associated with occurrences of quartz and/or pyrite veining occurring at lowermost levels (Fig. 7e). Notably, late stage epithermal-style veining and feldspar porphyry dykes were not observed to crosscut the Amadeus stock, suggesting stock emplacement was coeval with, or post-dated, the epithermal and dyking events observed in the Nightmusic zone. A sample of the Amadeus stock was collected for U-Pb geochronology.

GEOCHRONOLOGY

Four intrusive samples were collected from the Sonora Gulch property in order to place maximum and minimum age constraints on magmatism and related mineralization within both the Nightmusic and Amadeus zones. Sample preparation and U-Pb Laser Ablation Microprobe Inductively Coupled Plasma Mass Spectrometry (LAM ICP-MS) geochronology was completed at the Earth Sciences Department and the INCO Innovation Centre, Memorial University, St Johns', Newfoundland. A detailed outline of the methodology is given in Bennett and Tubrett (this volume). Analytical techniques used to characterize the zircon populations included standard optical microscopy and backscattered electron imaging (BSE) and cathodoluminescence (CL) image analysis in order to permit greater understanding of zircon zoning and growth history. Image analysis was completed on all zircon grains selected (n = 20-80, depending on yield). Field relationships and zircon zonation styles are briefly described for each sample before reporting the U-Pb isotopic results. Final interpreted crystallization ages are based on calculation of concordia ages from individual U-Pb isotopic analyses that have a probability of concordance greater than 0.20 (see Bennett and Tubrett, this volume). Weighted mean $^{206}Pb/^{238}U$ ages are also reported, to remain consistent with current U-Pb

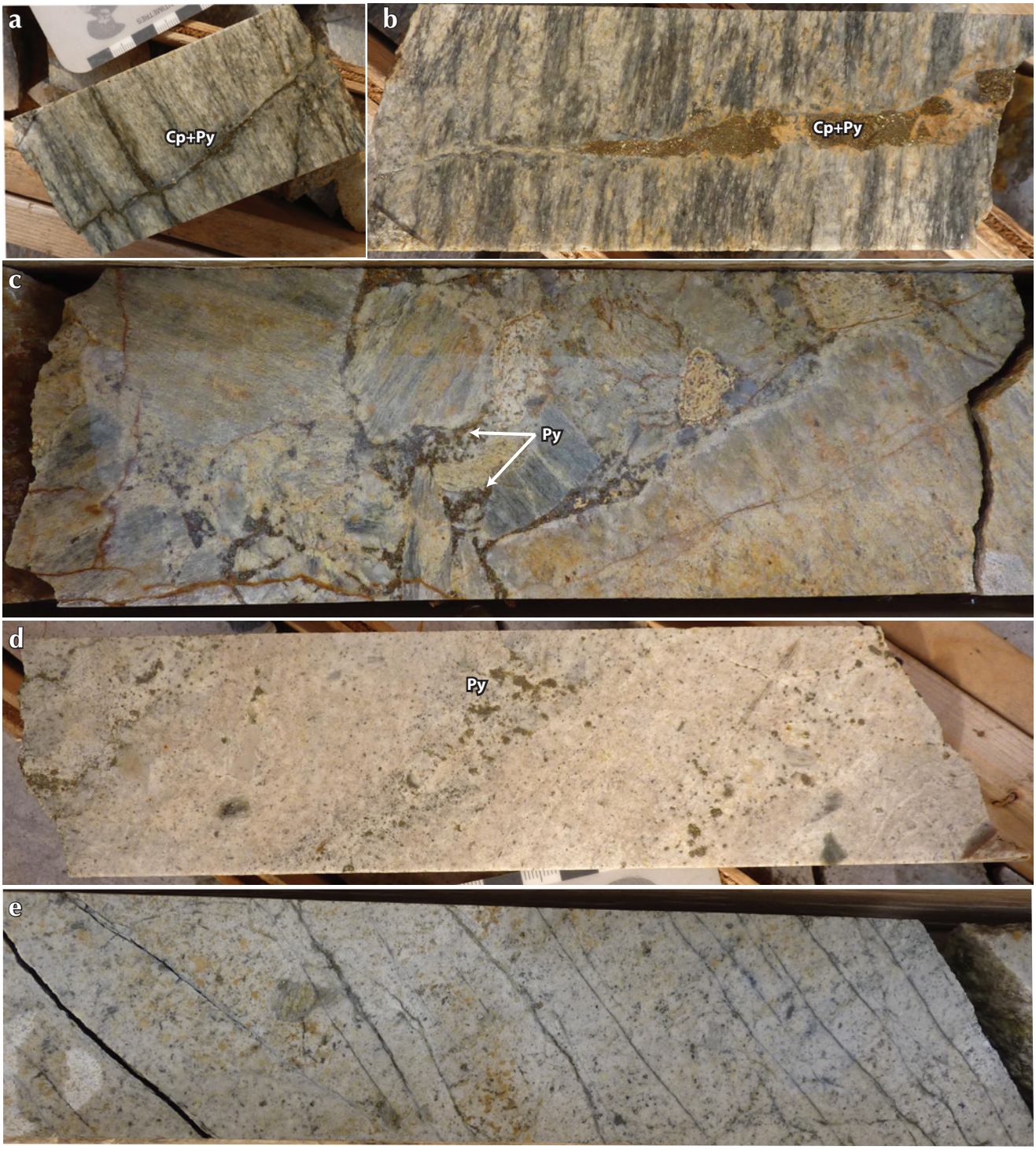

Figure 7. *Styles of mineralization occurring in the Amadeus stock, Amadeus zone (SG-08-31).* ***(a)*** *and* ***(b)*** *vein-hosted pyrite + chalcopyrite mineralization in basement granitic gneisses immediately above contact with Amadeus stock.* ***(c)*** *Intrusive breccia texture, contact zone, Amadeus stock.* ***(d)*** *Example of high-level Au mineralized zone in feldspar porphyry stock, Amadeus zone.* ***(e)*** *Example of lower level Ag mineralized zone, Amadeus stock. Cp = chalcopyrite, Py = pyrite.*

geochronology reporting trends. Two sigma uncertainty levels are reported for all calculated ages and plotted on concordia and weighted mean diagrams, unless stated otherwise. Final age calculations include U decay constant uncertainties, which are plotted graphically on concordia plots. Concordia and weighted mean $^{206}Pb/^{238}U$ ages were calculated using Ludwig (1999). The concordia age that includes U decay constant uncertainties is considered the best estimate of the crystallization age of a sample (see Bennett and Tubrett, this volume). Where a concordia age has a mean square of weighted deviates (MSWD) >1.5, the weighted mean $^{206}Pb/^{238}U$ age is considered the best estimate of the crystallization age. Uranium and thorium concentration data and Th/U ratios were also calculated for each sample.

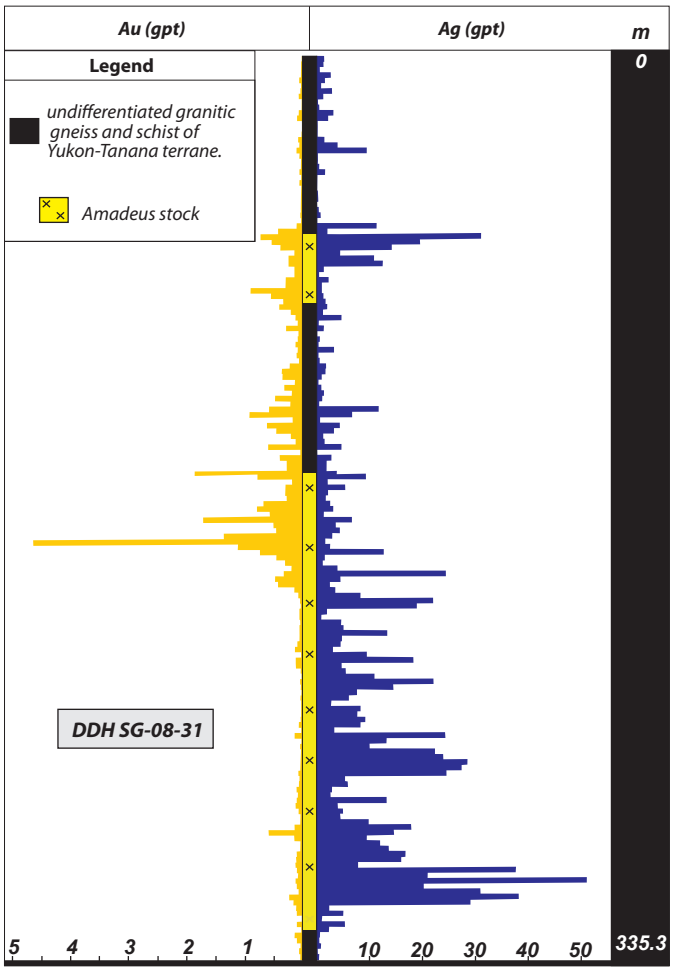

Figure 8. *Schematic drill log of DDH SG-08-31, illustrating vertical zonation trends in Au and Ag mineralization (gpt) within the high-level Amadeus stock. Economic concentrations of Au occur at higher levels of the intrusion and Ag increases in concentration at lowermost levels. Modified after Northern Tiger Resources 2008 assessment report, drill log DDH SG-08-31.*

NIGHTMUSIC ZONE

Three magmatic samples were collected from the Nightmusic zone, including a weakly mineralized, quartz feldspar granitic porphyry stock (NTR-1) sampled from the historical gold vein system, and two feldspar porphyry dykes sampled from both drill core (DDH SG-09-41) and from surface within Nightmusic zone (Road FP dyke).

Sample NTR-1, QFP Stock (UTM 651779E 6949756N, NAD 83 Zone 7)

Weak to moderately pyritic quartz-feldspar granite was sampled approximately 300 m north of the current site of Northern Tiger Resources' Sonora Gulch summer exploration camp, within the historical gold vein system for which the Sonora Gulch area was initially staked in 1965. The stock has a porphyritic texture with smoky to clear quartz eyes, feldspar phenocrysts and lesser biotite (Davidson, 2000; Fig. 9a-c). Argillic and propylitic alteration and abundant quartz veining occur in mineralized portions of the stock. The U-Pb sample site was located in a relatively unaltered part of the stock (Fig. 9a).

The U-Pb sample yielded abundant zircon grains of poor to moderate quality. Two morphologically distinct populations are present: subordinate, clear to turbid prisms (Fig. 9d) and abundant elongate bipyramidal prisms with colourless, translucent overgrowths (Fig. 9e). Backscattered electron and CL imaging of both zircon populations demonstrate magmatic zircon occurs as both entire grains, and as rims of partially resorbed xenocrystic cores. In either case, magmatic zircon growth is characterized by sharp oscillatory growth zoning. Clear truncation of xenocrystic cores is a striking feature characterizing zircon within the NTR-1 sample (Fig. 10).

Twenty-three analyses were collected from 18 magmatic rims and 5 xenocrystic cores (Fig. 11, Appendix 1). A concordia age calculated from 18 rim analyses yielded an age of 75.73 ± 0.93 Ma (MSWD = 0.0020) and a weighted mean $^{206}Pb/^{238}U$ age of 75.75 ± 0.96 Ma (MSWD = 0.27; Fig. 11a,b). Xenocrystic core analyses yielded 3 different age populations including *ca.* 85 Ma, 104 Ma and 410 Ma (Appendix 1). Concentration data calculated from magmatic zircon varies from 223-2250 ppm U and 75-427 ppm Th (Appendix 1); Th/U ratios calculated for all zircon analyses highlight the

Figure 9. ***(a)*** *U-Pb sampling locality for NTR-1, QFP stock.* ***(b)*** *Weakly mineralized (Py ± Po) QFP stock adjacent to sampling locality.* ***(c)*** *Slab image of U-Pb sample, NTR-1. Scale bar represents 1 cm. Transmitted light images of* ***(d)*** *zircon prism population and* ***(e)*** *zircon overgrowth, bipyramid population from NTR-1, QFP stock. Scale bars in d and e represent 50 μm.*

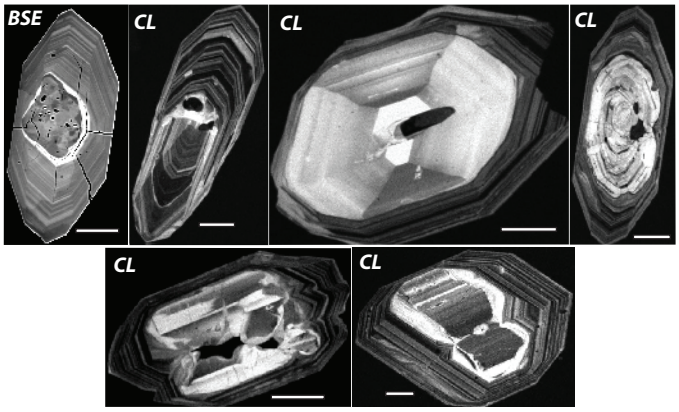

Figure 10. *Representative BSE and CL images (denoted on image) of analysed zircon grains from NTR-1, QFP stock. Images demonstrate complex xenocrystic core and magmatic rim relationships. Magmatic rims exhibit fine, well defined, oscillatory zones enclosing partially resorbed xenocrystic cores. Scale bars represent 50 μm.*
BSE = backscattered electron, CL = cathodoluminescence.

difference in zircon chemistry between xenocrystic cores and magmatic rims, notably due to the higher U content associated with magmatic zircon (Fig. 11c).

Feldspar porphyry dykes

Several feldspar porphyry dykes occur in both drill core and at surface within the Nightmusic zone. The dykes are typically weakly mineralized (Py) and commonly associated with pervasive limonite alteration and vein halo potassic alteration (Figs. 6 and 12). Minor late-stage chalcedonic veining exhibiting open space-filling epithermal textures, overprint the porphyry dykes (Fig. 6c). A series of feldspar porphyry dykes were intersected in DDH SG-09-41 at a depth that intersected the Big Creek fault. A single dyke was sampled between the interval 152.8-153.3 m (Fig. 12a,b). A second feldspar porphyry dyke was sampled on surface at the western margin of the Nightmusic zone, immediately adjacent to the surface trace of the Big Creek fault (Figure 12e; 652238E 6950372N, NAD 83 Zone 7).

Nineteen zircon grains were extracted from the porphyry dyke sampled from DDH SG-09-41. Zircon populations consisted of: (i) elongate needles and prisms with small, well-faceted overgrowths; and (ii) a subordinate population of large broken and fractured grains with indistinct crystal terminations (Fig. 12c,d). The porphyry dyke sampled at surface yielded abundant zircon grains of moderate to high quality that were subdivided into three morphologically distinct populations: (i) minor translucent, well-faceted, elongate to equidimensional prisms; (ii) abundant elongate prisms with optically distinct core and rim relationships; and (iii) elongate bipyramidal prisms with thin colourless and

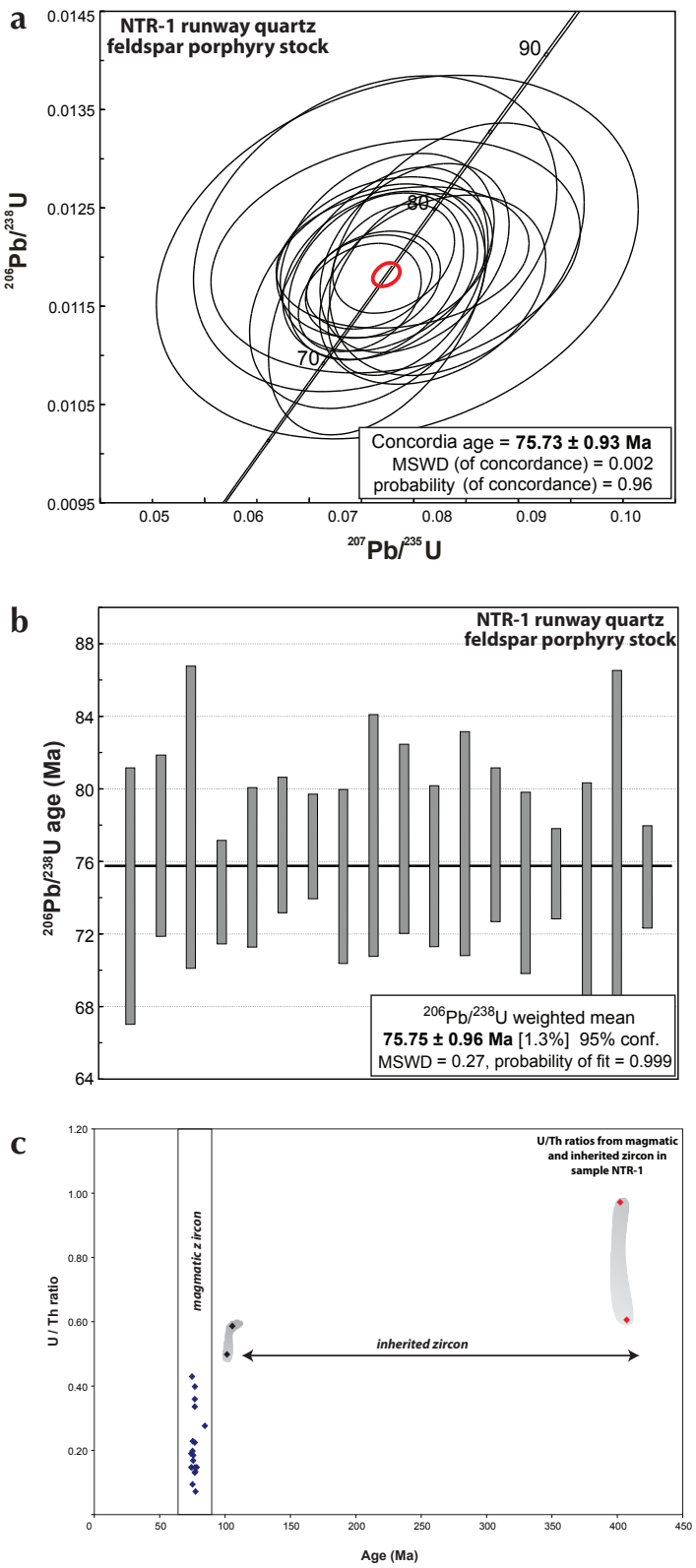

Figure 11. ***(a)*** *Concordia diagram for U-Pb analyses of magmatic zircon from NTR-1, QFP stock. Analyses included in age calculation have a probability of concordance greater than 0.20.* ***(b)*** *Plot of weighted mean $^{206}Pb/^{238}U$ ages with probability of concordance greater than 0.20.* ***(c)*** *Plot of U/Th ratio for magmatic and inherited zircon illustrating chemical variation between magmatic zircon and xenocrystic cores. Notes: 1. On all diagrams, MSWD = mean square of the weighted deviates; 2. On all U-Pb concordia diagrams, data point error ellipses represent 2σ error and 2σ uranium decay constant errors are included in final age calculation; 3. On all weighted mean $^{206}Pb/^{238}U$ diagrams, box heights represent 2σ.*

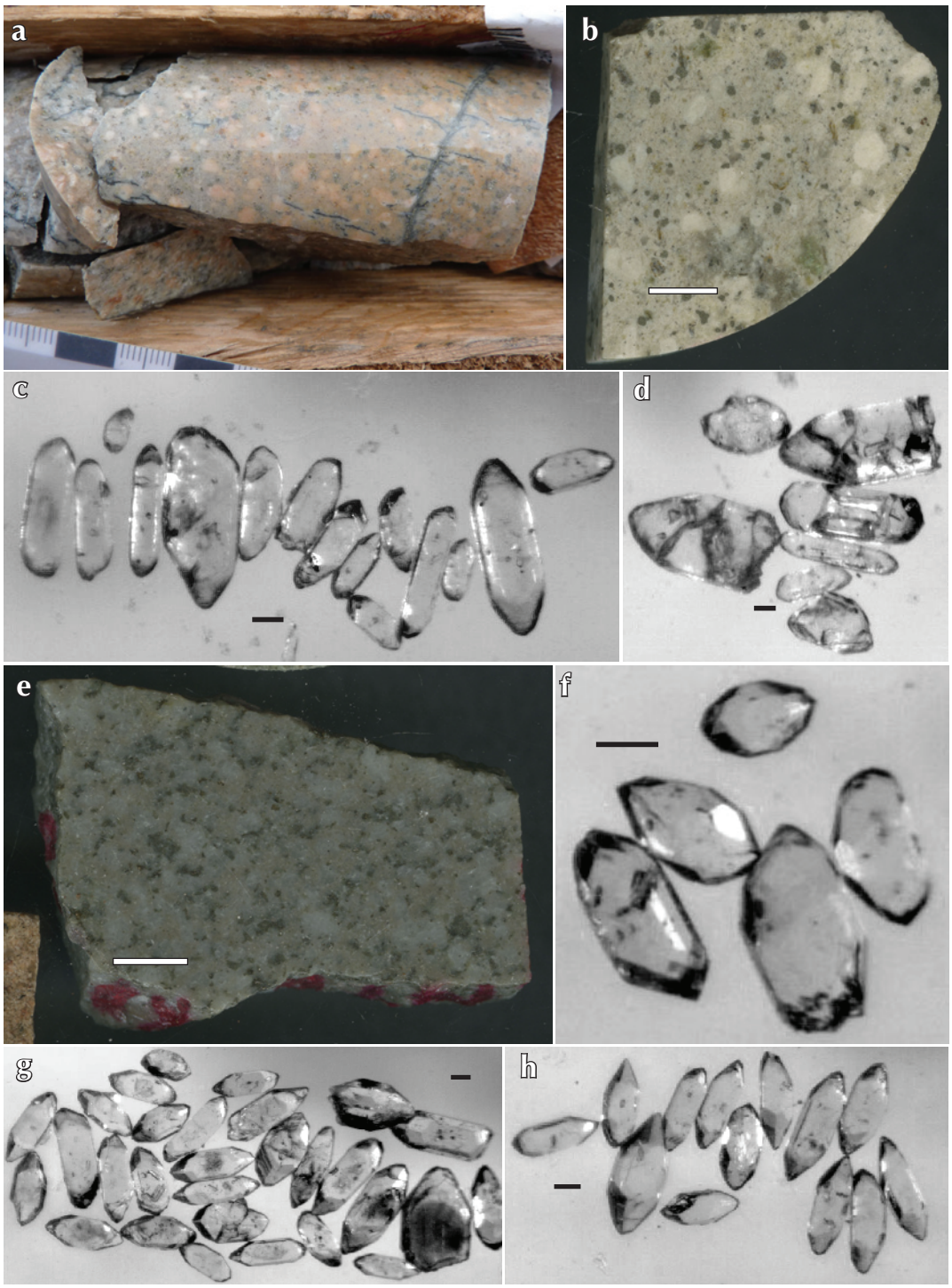

Figure 12. ***(a)*** *Core photo illustrating vein-hosted sulphide mineralization and associated alteration halo within feldspar porphyry dyke, DDH SG-09-41.* ***(b)*** *Slab image of feldspar porphyry dyke, U-Pb sample. Scale bar represents 1 cm. Transmitted light images of* ***(c)*** *needle and elongate zircon prism population with overgrowths and* ***(d)*** *irregular large fractured grains. Scale bar represents 50 μm.* ***(e)*** *Slab image of feldspar porphyry dyke, U-Pb sample occurring at surface in Nightmusic zone. Scale bar represents 1 cm. Transmitted light images of* ***(f)*** *large, equidimensional prism zircon population,* ***(g)*** *complex core-rim zircon grains, and* ***(h)*** *prismatic bipyramidal zircon population. Scale bar represents 50 μm.*

translucent overgrowths (Fig. 12f-h). Backscattered electron and CL imaging of zircon grains in feldspar porphyry dyke samples demonstrates magmatic zircon occurs as entire grains and as rims mantling xenocrystic cores (Fig. 13). Magmatic zircon in both samples is characterized by well-defined, sharp oscillatory growth zoning.

Twenty-four analyses were acquired from 15 zircon grains exhibiting magmatic growth zoning from the feldspar porphyry dyke sampled from DDH SG-09-41, (Fig. 14a; Appendix 2). A concordia age calculated from 22 analyses yielded an age of 74.64 ± 0.61 Ma (MSWD = 1.6) and a weighted mean $^{206}Pb/^{238}U$ age of 74.79 ± 0.61 Ma (MSWD = 0.47; Figure 14a,b). Concentration data calculated for magmatic zircon ranges from 162-1637 U ppm and 50-242 ppm Th (Appendix 2).

For the feldspar porphyry sampled at surface from the Nightmusic zone, 24 analyses were collected from 19 grains (Fig. 14c; Appendix 3). A concordia age calculated from 17 analyses yielded an age of 74.42 ± 0.75 Ma (MSWD = 2.4) and a weighted mean $^{206}Pb/^{238}U$ age of 73.91 ± 0.81 Ma (MSWD = 0.5; Fig. 14c,d). Concentration data calculated for magmatic zircon vary from 170-2772 ppm U and 29-323 ppm Th (Appendix 3).

AMADEUS ZONE

Amadeus stock (DDH SG-08-32)

The Amadeus stock represents an epithermal quartz-feldspar porphyry intrusion and hosts significant Au-Ag mineralization. The stock is characterized by pervasive bleaching and primary zoned plagioclase phenocrysts

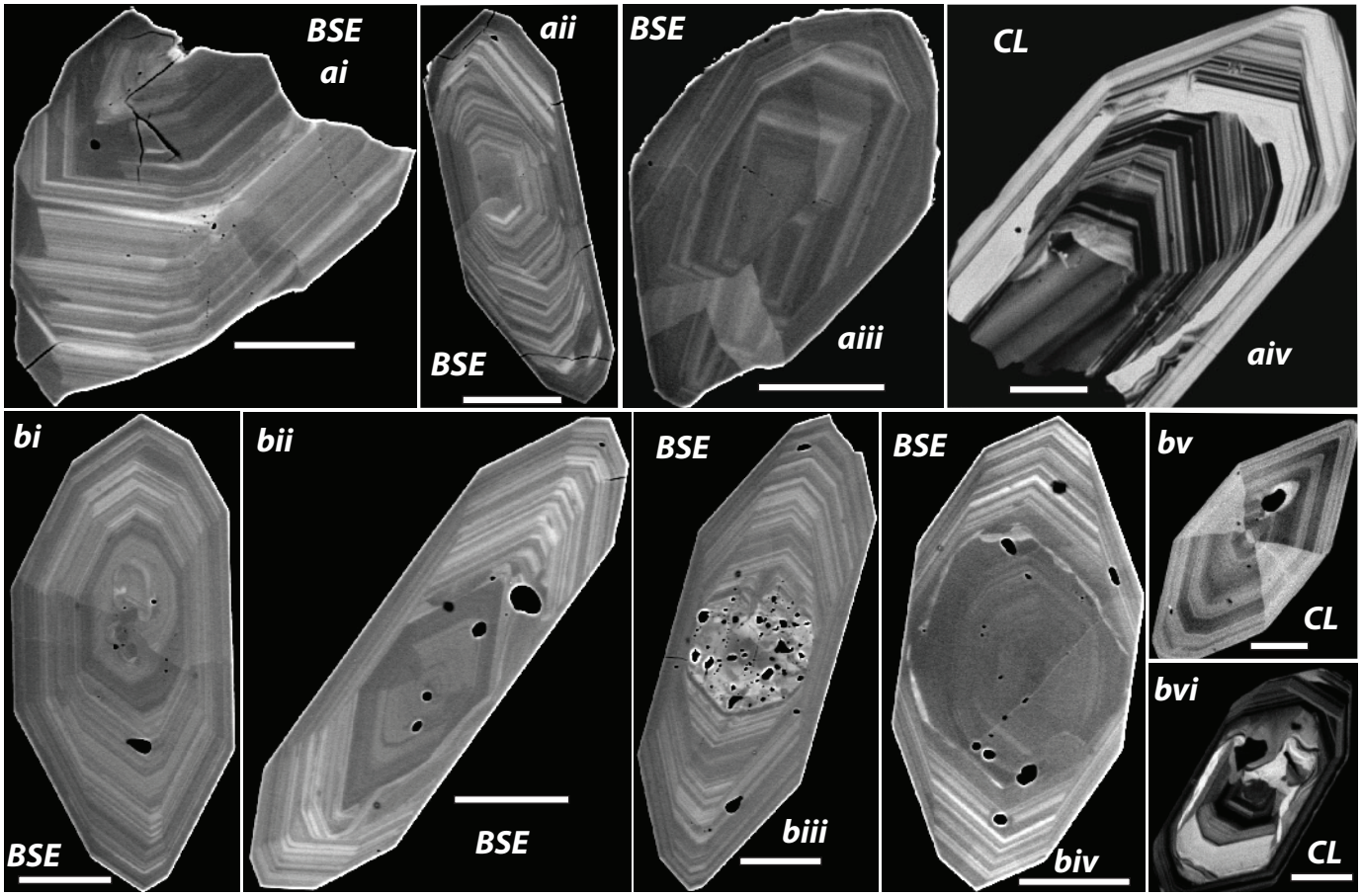

Figure 13. (ai-aiv) *Representative BSE and CL images (denoted on image) of analysed zircon grains from feldspar porphyry dyke sampled from SG-09-41. Zircon grain in image 13(aiv) exhibits prominent oscillatory-zoned magmatic rims enclosing a partially resorbed xenocrystic core.* ***(bi-bvi)*** *Representative BSE and CL images (denoted on image) of analysed zircon grains from feldspar porphyry dyke sampled at surface within Nightmusic zone. Magmatic zircon is characterized by oscillatory zoning occurring either as rims on xenocrystic cores or as entire grains. Scale bars represent 50 μm. BSE = backscattered electron, CL = cathodoluminescence.*

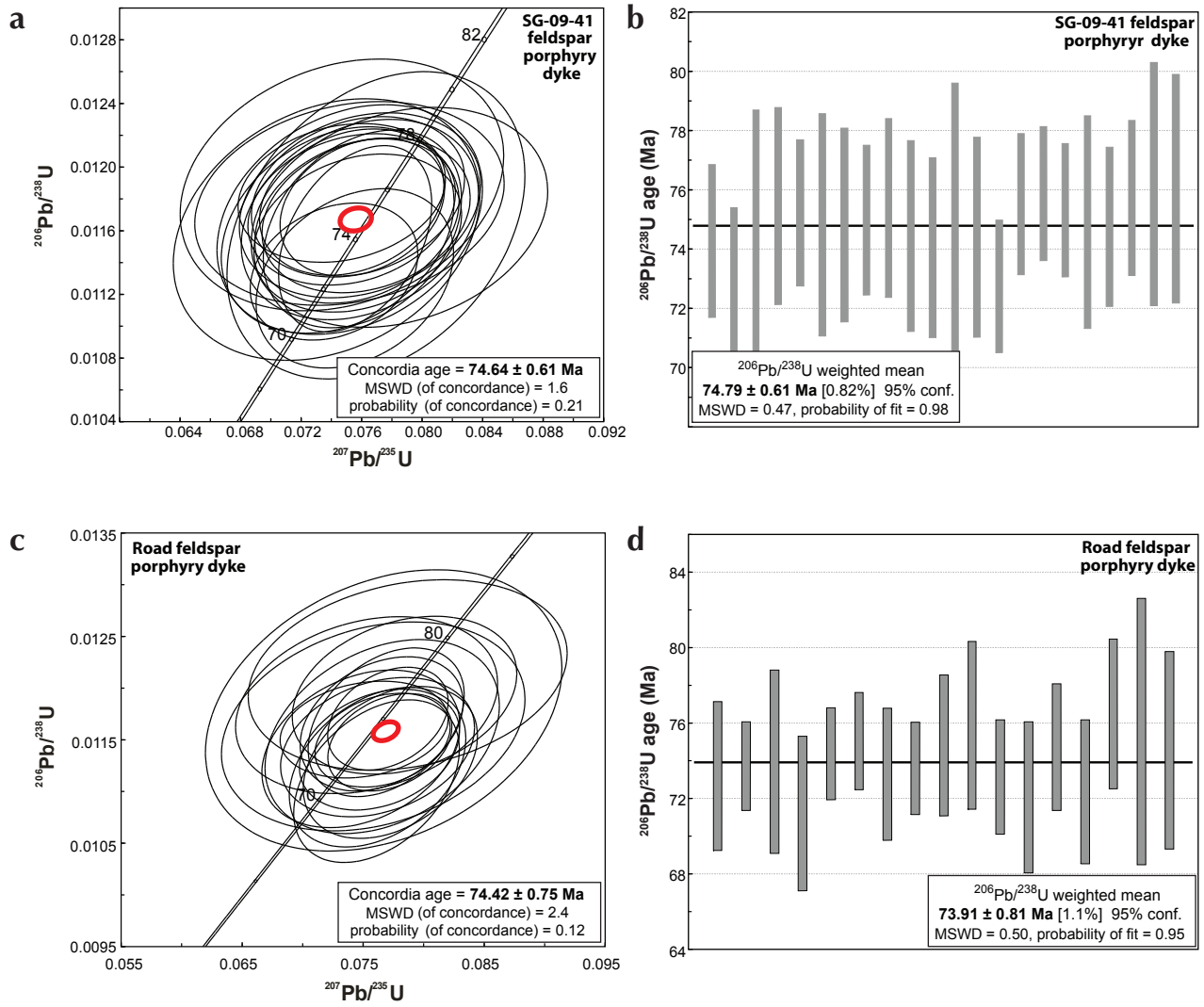

Figure 14. ***(a)*** *Concordia diagram illustrating U-Pb analyses of magmatic zircon from feldspar porphyry dyke sampled from DDH SG-09-41 (ca. 152.8-153.3 m). Analyses included in age calculation have a probability of concordance greater than 0.20. Decay constant uncertainties of concordia are indicated.* ***(b)*** *Plot of weighted mean $^{206}Pb/^{238}U$ ages with probability of concordance greater than 0.20 for feldspar porphyry dyke, DDH SG-09-41.* ***(c)*** *Concordia diagram illustrating U-Pb analyses of magmatic zircon from feldspar porphyry dyke sampled at surface within the Nightmusic zone. Analyses included in age calculation have a probability of concordance greater than 0.20.* ***(d)*** *Plot of weighted mean $^{206}Pb/^{238}U$ ages with probability of concordance greater than 0.20 for surface sample of feldspar porphyry dyke, Nightmusic zone.*

that have been completely replaced by secondary clay minerals, particularly in Au-enriched portions of the intrusion (Fig. 15a,b). Xenoliths of metasedimentary and meta-igneous gneiss occur sporadically throughout the body, and are particularly abundant along upper and lower contacts, which are typically brecciated (Fig. 15c,d). Sampling for U-Pb geochronology was restricted to xenolith-free portions of the stock that displayed clear magmatic textures from DDH SG-08-32 (272.2-300.4 m; Fig. 15b).

Abundant zircon of moderate quality was extracted from the sample of the Amadeus stock. Two morphologically distinct populations are present in subequal amounts, including (i) clear, well-faceted elongate prisms and needles (Fig. 15c), and (ii) elongate prisms with core and rim relationships (Fig. 15f). Backscattered electron and CL imaging of both zircon populations demonstrate magmatic zircon occurs both as entire grains and as thick magmatic rims. Magmatic zircon is characterized by sharp oscillatory zoning (Fig. 16).

Twenty-seven analyses were acquired from 25 grains that were interpreted as magmatic zircon (Appendix 3). A concordia age calculated from 18 analyses yielded an age of 75.5 ± 0.79 Ma (MSWD = 1.07) and a weighted mean $^{206}Pb/^{238}U$ age of 75.53 ± 0.89 Ma (MSWD = 0.48; Figure 17a,b). Concentration data calculated from magmatic zircon ranges from 718-2608 ppm U and 92-796 ppm Th (Appendix 3).

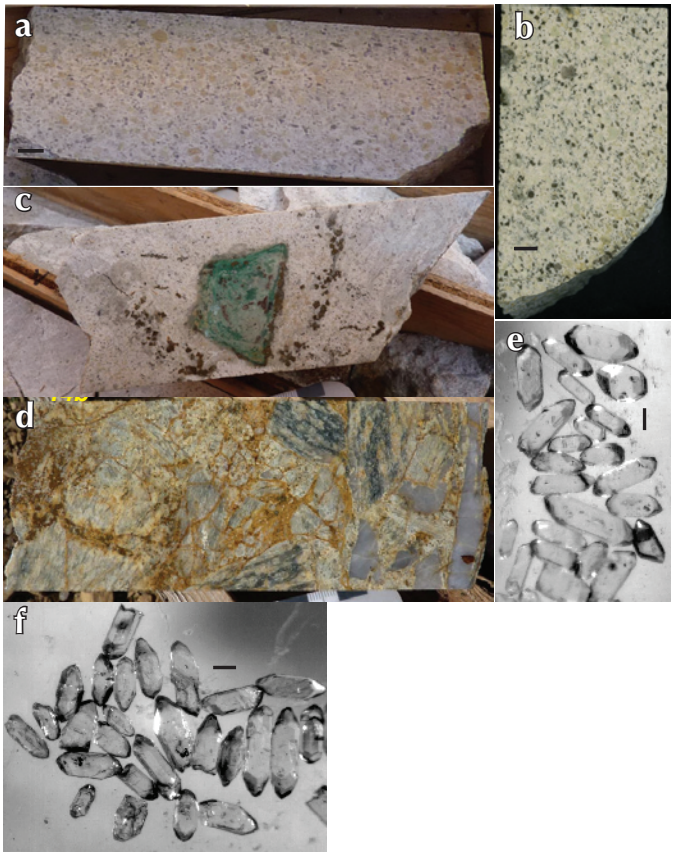

Figure 15. ***(a)*** *Core photo illustrating feldspar porphyritic texture of medium to coarse-grained feldspar porphyry stock (Amadeus stock) sampled from DDH SG-08-32 (272.2-300.4 m). Scale bar represents 1 cm.* ***(b)*** *Slab image of U-Pb sample. Scale bar represents 1 cm.* ***(c)*** *Listwanite-altered ultramafic inclusion within Amadeus stock.* ***(d)*** *Brecciated upper contact of Amadeus stock with basement gneiss of Yukon-Tanana terrane. Transmitted light images of* ***(e)*** *faceted to prismatic zircon population, and* ***(f)*** *overgrowth zircon population. Scale bars represent 50 μm.*

DISCUSSION AND CONCLUSIONS

New geological, geophysical and U-Pb analytical data from the Sonora Gulch project indicate the occurrence of multiple overprinting events that can be correlated to different mineralizing environments (mesothermal *vs.* epithermal) and metal associations. Important vectoring criteria for the Nightmusic zone include proximity to the

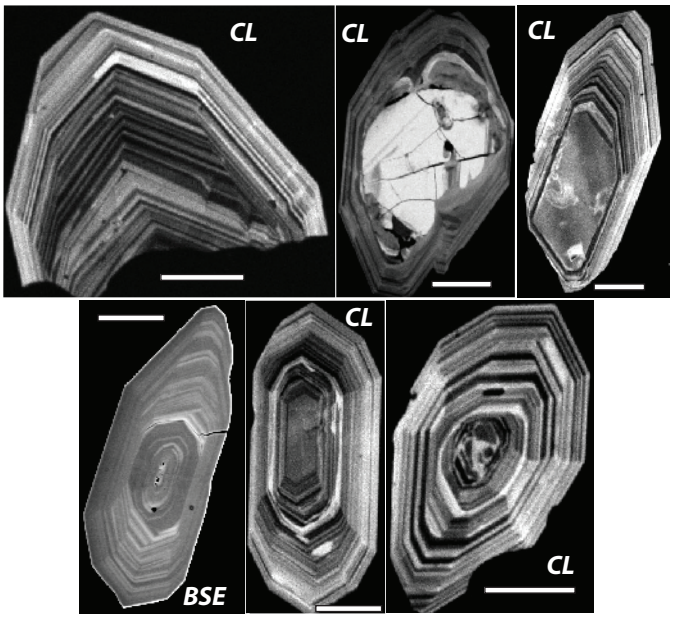

Figure 16. *Representative BSE and CL images (denoted on image) of analysed zircon grains from Amadeus stock. Magmatic rims exhibit oscillatory enclosing partially resorbed xenocrystic cores. Scale bars represent 50 μm.*

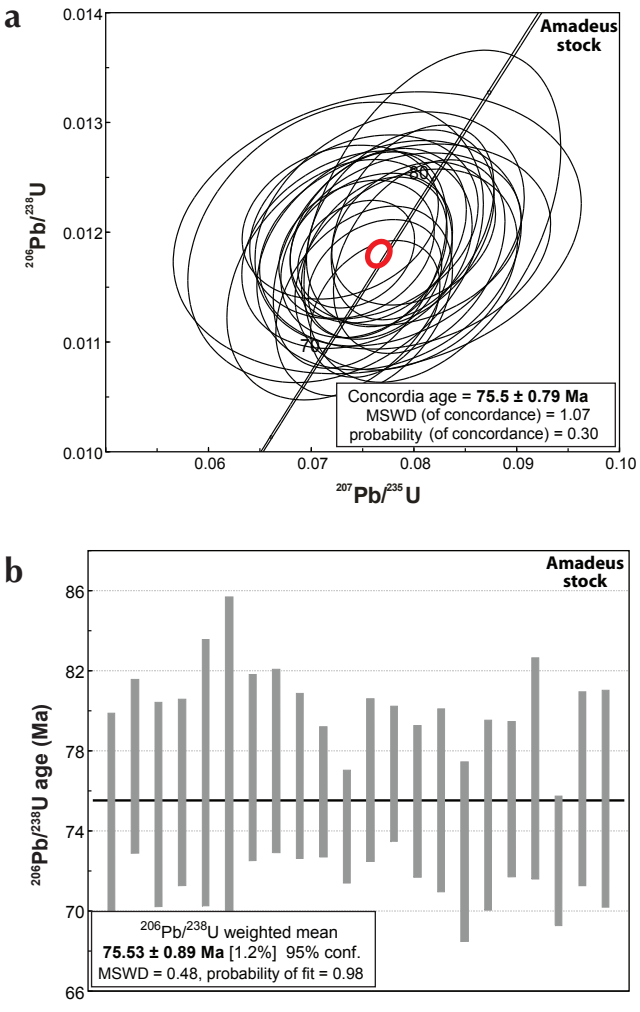

Figure 17. ***(a)*** *Concordia diagram illustrating U-Pb analyses of magmatic zircon from Amadeus stock. Analyses included in age calculation have a probability of concordance greater than 0.20. Decay constant uncertainties of concordia are indicated.* ***(b)*** *Plot of weighted mean $^{206}Pb/^{238}U$ ages with probability of concordance greater than 0.20 for Amadeus stock.*

northwest-trending Big Creek fault zone and recognition of an associated second-order, east-trending structural corridor. Serpentinized and listwanite-altered ultramafic lenses provide useful lithologies to focus on important target areas in this structural setting. Gold-enriched mesothermal base-metal skarn and replacement-style mineralization in the Nightmusic zone is overprinted by post-skarn fluid and magmatic events, including ubiquitous epithermal veining, feldspar porphyry dyke suite intrusion. Additionally, skarn sulphide paragenesis indicates replacement of sphalerite-galena-chalcopyrite (± Au) mineralization by secondary pyrite and pyrrhotite, which may represent either the latest stage of skarn fluid evolution, or a discretely different fluid event that remobilized the pre-existing ore. Gold and silver mineralization occurring in the Amadeus stock show vertical zonation with appreciable concentrations of gold occurring at higher levels and silver at lower levels. Intervals of higher grade gold are typically associated with low to background arsenic values, suggesting a more evolved epithermal nature of gold mineralization.

The new U-Pb age data determined from each of two feldspar porphyry dykes (74.79 ± 0.61 Ma and 73.91 ± 0.81 Ma), a weakly mineralized quartz porphyry stock (75.73 ± 0.93 Ma) within the Nightmusic zone, and the gold-silver mineralized Amadeus stock (75.5 ± 0.79 Ma) demonstrate the widespread occurrence of Late Cretaceous magmatism within the property. This magmatism is coeval with the Late Cretaceous Carmacks Group rather than the mid-Late Cretaceous Prospector Mountain suite as previously interpreted. Age dating of a feldspar porphyry dyke located in the Nightmusic zone and occurring within the Big Creek fault zone, indicates that brittle deformation and movement along the Big Creek fault post-dated dyke emplacement (*ca.* 74 Ma). The age data also indicate that mineralization styles evolved from early mesothermal replacement and skarn type (Nightmusic zone), to a younger epithermal mineralizing environment, with the most economic concentrations currently recognized as occurring within the Amadeus zone. The lack of late-stage epithermal-style veining or feldspar porphyry dyke emplacement within the Amadeus stock is consistent with U-Pb age data that indicate that stock and dyke emplacement were contemporaneous.

Importantly, the new age dates indicate that magmatic-associated mineralization occurring within the Sonora Gulch property area are temporally equivalent to Western Copper Corporation's Casino Cu-Au-Mo deposit, located roughly 40 km to the west-northwest. Hence, these new datasets extend the currently known eastern limit of Late Cretaceous magmatism and associated polymetallic mineralization.

ACKNOWLEDGEMENTS

We thank Pam King, Earth Sciences Department, and Michael Tubrett and Michael Schaeffer for access and assistance in the MafIIC analytical facility, Memorial University. An earlier draft of this paper was reviewed and improved by Maurice Colpron.

REFERENCES

Bennett, V. and Tubrett, M., 2010. U-Pb Isotopic Age dating by LAM ICP-MS, INCO Innovation Centre, Memorial University: Sample preparation methodology and analytical techniques. *In:* Yukon Exploration and Geology 2009, K.E. MacFarlane, L.H. Weston and L.R. Blackburn (eds.), Yukon Geological Survey, p. 47-55.

Bineli Betsi, T. and Bennett, V., 2010. New U-Pb age constraints at Freegold Mountain: evidence for multiple phases of polymetallic mid- to Late Cretaceous Mineralization. *In:* Yukon Exploration and Geology 2009, K.E. MacFarlane, L.H. Weston and L.R. Blackburn (eds.), Yukon Geological Survey, p. 57-84.

Colpron, M., Nelson, J.L. and Murphy, D.C., 2006. A tectonostratigraphic framework for the pericratonic terranes of the northern Cordillera. *In:* Paleozoic Evolution and Metallogeny of Pericratonic Terranes at the Ancient Pacific Margin of North America, M. Colpron and J.L. Nelson (eds.), Geological Association of Canada, Special Paper 45, p. 1-23.

Davidson, G.S., 2000. Summary Report on the Sonora Gulch Property. Private report for Engineer Mining Corporation.

Gordy, S.P. and Makepeace, A.J., 1999. Yukon Digital Geology. Geological Survey of Canada, Open File D3826. Exploration and Geological Services Division, Yukon, Indian and Northern Affairs Canada, Open File 1999-1(D).

Johnston, S.T. and Hachey, N., 1993. Preliminary Results of 1:50 000 Scale Geologic Mapping in Wolverine Creek Map Area (115I-12), Dawson Range, Southwest Yukon. *In:* Yukon Exploration and Geology 1992, Exploration and Geological Services Division, Yukon Region, Indian and Northern Affairs Canada, p. 49-60.

Ludwig, K.R., 1999. User's manual for Isoplot/Ex, version 2.06: a geochronological toolkit for Microsoft Excel. Berkeley Geochronological Center, Special Publication No. 1a, 49 p.

Mortensen, J.K., 1992. Pre-mid-Mesozoic tectonic evolution of the Yukon-Tanana terrane, Yukon and Alaska. Tectonics, vol. 11, p. 836-853.

Mortensen, J.K., Appel, V.L. and Hart, C.J.R., 2003. Geological and U-Pb age constraints on base and precious metal vein systems in the Mount Nansen area, eastern Dawson Range, Yukon. *In:* Yukon Exploration and Geology 2002, D.S. Emond and L.L. Lewis (eds.), Exploration and Geological Services Division, Yukon Region, Indian and Northern Affairs Canada, p. 165-174.

Schulze, C. 2004: Summary and Preliminary Exploration Report on the Sonora Gulch Property, Dawson Range, Yukon; NI 43-101 Compatible Report for Firestone Ventures Inc. Effective date of report completion, April 14, 2004. Downloaded from SEDAR <*http://www.sedar.com*>, December, 2009.

Schulze, C., 2007a: Assessment Report, 2006 Geological, Geophysical and Diamond Drilling Programs on the Sonora Gold Project, Carmacks area, Yukon Territory, Canada. Ministry of Energy, Mines and Resources, Government of Yukon.

Schulze, C. 2007b. NI 43-101 technical report on the 2006 and 2007 exploration programs, Sonora Property, Dawson Range, Yukon, 279 p. Effective date of report completion, October 15, 2007. Downloaded from SEDAR <*http://www.sedar.com*>, July, 2009.

Tempelman-Kluit, D.J., 1984. Geology of the Laberge (105E) and Carmacks (115I) map areas. Geological Survey of Canada, Open File 1101, 1:250 000 scale.

Appendix 1. *LAM ICP-MS U-Pb analytical data for magmatic and inherited zircon from NTR-1, runway stock.*

	Measured isotopic ratios							Calculated ages										
Analysis	$^{207}Pb/^{235}U$	1σ err.	$^{206}Pb/^{238}U$	1σ err.	Rho	$^{207}Pb/^{206}Pb$	1σ err.	$^{207}Pb/^{235}U$ Ma	1σ err. Ma	$^{206}Pb/^{238}U$ Ma	1σ err. Ma	Conc. age (Ma)	2σ err. Ma	MSWD of conc.	Prob. of conc.	Th ppm	U ppm	Ratio Th/U
Magmatic zircon																		
oc15B92	0.0766	0.0043	0.0116	0.0006	0.4303	0.0487	0.0004	75	4	74	4	74	6	0.05	0.82	427	2250	0.19
oc15B93	0.0801	0.0037	0.0120	0.0004	0.3551	0.0491	0.0007	78	3	77	3	77	5	0.16	0.69	119	530	0.22
oc15B94	0.0763	0.0071	0.0122	0.0007	0.2883	0.0467	0.0009	75	7	78	4	78	8	0.30	0.58	198	1342	0.15
oc15B96	0.0748	0.0024	0.0116	0.0002	0.3025	0.0477	0.0005	73	2	74	1	74	3	0.19	0.66	245	1666	0.15
oc15B97	0.0764	0.0034	0.0118	0.0003	0.3291	0.0482	0.0007	75	3	76	2	75	4	0.07	0.79	143	852	0.17
oc15B98	0.0789	0.0049	0.0120	0.0003	0.1958	0.0508	0.0013	77	5	77	2	77	4	0.00	0.95	75	223	0.34
oc15B99	0.0781	0.0024	0.0120	0.0002	0.3105	0.0480	0.0005	76	2	77	1	77	3	0.04	0.84	126	968	0.13
oc15B100	0.0793	0.0031	0.0117	0.0004	0.4163	0.0494	0.0005	77	3	75	2	76	4	0.67	0.41	279	1408	0.20
oc15B101	0.0841	0.0050	0.0121	0.0005	0.3672	0.0497	0.0007	82	5	77	3	79	6	0.99	0.32	122	1708	0.07
oc15B106	0.0775	0.0042	0.0120	0.0004	0.3162	0.0478	0.0006	76	4	77	3	77	5	0.13	0.72	114	852	0.13
oc15B107	0.0768	0.0038	0.0118	0.0003	0.2979	0.0488	0.0005	75	4	76	2	76	4	0.03	0.87	226	1225	0.18
oc15B108	0.0783	0.0072	0.0120	0.0005	0.2194	0.0521	0.0011	77	7	77	3	77	6	0.00	0.95	170	427	0.40
oc15B111	0.0772	0.0042	0.0120	0.0003	0.2549	0.0470	0.0008	76	4	77	2	77	4	0.12	0.73	160	446	0.36
oc15B112	0.0818	0.0044	0.0117	0.0004	0.3116	0.0510	0.0007	80	4	75	3	76	5	1.51	0.22	233	543	0.43
oc15B114	0.0758	0.0025	0.0117	0.0002	0.2564	0.0493	0.0005	74	2	75	1	75	2	0.23	0.63	283	1239	0.23
oc15B116	0.0756	0.0046	0.0116	0.0005	0.3299	0.0488	0.0006	74	4	74	3	74	6	0.01	0.93	133	909	0.15
oc15B117	0.0784	0.0094	0.0120	0.0008	0.2622	0.0515	0.0007	77	9	77	5	77	9	0.00	0.98	192	1306	0.15
oc15B118	0.0761	0.0026	0.0117	0.0002	0.2738	0.0472	0.0007	74	2	75	1	75	3	0.06	0.80	93	994	0.09
Inherited zircon																		
oc15B95	0.5017	0.0163	0.0652	0.0013	0.2962	0.0559	0.0007	413	11	407	8	409	14	0.25	0.61	101	167	0.61
oc15B109	0.1046	0.0056	0.0165	0.0005	0.2858	0.0473	0.0007	101	5	106	3	105	6	0.76	0.38	339	578	0.59
oc15B110	0.0872	0.0070	0.0132	0.0004	0.2045	0.0484	0.0010	85	7	85	3	85	5	0.00	0.96	101	365	0.28
oc15B113	0.1056	0.0065	0.0159	0.0007	0.3463	0.0485	0.0007	102	6	102	4	102	8	0.00	0.95	346	694	0.50
oc15B115	0.5349	0.1798	0.0644	0.0093	0.2144	0.0577	0.0010	435	119	402	56	406	109	0.07	0.79	413	425	0.97

Appendix 2. *LAM ICP-MS U-Pb analytical data for magmatic zircon from diamond drillhole SG-09-41 feldspar porphyry dyke and Road feldspar porphyry dyke.*

	Measured isotopic ratios							Calculated ages										
Analysis	$^{207}Pb/^{235}U$	1σ err.	$^{206}Pb/^{238}U$	1σ err.	Rho	$^{207}Pb/^{206}Pb$	1σ err.	$^{207}Pb/^{235}U$ Ma	1σ err. Ma	$^{206}Pb/^{238}U$ Ma	1σ err. Ma	Conc. age (Ma)	2σ err. Ma	MSWD of conc.	Prob. of conc.	Th ppm	U ppm	Ratio Th/U
SG-09-41 - FP																		
oc15c166	0.07575	0.00281	0.01159	0.00020	0.23652	0.04926	0.00058	74	3	74	1	74	3	0.00	0.97	219	1371	0.16
oc15c167	0.07555	0.00267	0.01130	0.00023	0.28854	0.04959	0.00062	74	3	72	1	73	3	0.36	0.55	177	1113	0.16
oc15c168	0.07369	0.00414	0.01161	0.00034	0.25760	0.04567	0.00076	72	4	74	2	74	4	0.31	0.58	120	535	0.22
oc15c169	0.07520	0.00418	0.01177	0.00026	0.19989	0.05036	0.00084	74	4	75	2	75	3	0.21	0.65	100	482	0.21
oc15c170	0.07534	0.00280	0.01173	0.00019	0.22275	0.04916	0.00077	74	3	75	1	75	2	0.29	0.59	162	666	0.24
oc15c172	0.07522	0.00359	0.01167	0.00029	0.26497	0.04709	0.00086	74	3	75	2	75	4	0.12	0.73	71	398	0.18
oc15c173	0.07588	0.00320	0.01167	0.00026	0.26101	0.04890	0.00060	74	3	75	2	75	3	0.03	0.86	75	893	0.08
oc15c174	0.07630	0.00281	0.01170	0.00020	0.23063	0.04945	0.00056	75	3	75	1	75	2	0.01	0.91	112	1405	0.08
oc15c175	0.07589	0.00326	0.01176	0.00024	0.23501	0.04882	0.00073	74	3	75	2	75	3	0.12	0.72	189	859	0.22
oc15c176	0.07605	0.00268	0.01161	0.00025	0.31043	0.04700	0.00062	74	3	74	2	74	3	0.00	1.00	148	920	0.16
oc15c177	0.07557	0.00207	0.01155	0.00024	0.37819	0.04733	0.00041	74	2	74	2	74	3	0.00	0.98	83	1637	0.05
oc15c187	0.07695	0.00402	0.01163	0.00039	0.32438	0.04774	0.00071	75	4	75	3	75	5	0.03	0.85	113	669	0.17
oc15c188	0.07407	0.00273	0.01192	0.00020	0.22676	0.04756	0.00060	73	3	76	1	76	2	2.16	0.14	242	788	0.31
oc15c190	0.07442	0.00314	0.01160	0.00027	0.27042	0.04775	0.00064	73	3	74	2	74	3	0.25	0.62	89	710	0.13
oc15c191	0.07417	0.00227	0.01134	0.00018	0.25389	0.04846	0.00055	73	2	73	1	73	2	0.00	0.98	111	1305	0.09
oc15c194	0.07535	0.00249	0.01178	0.00019	0.24120	0.04780	0.00059	74	2	75	1	75	2	0.54	0.46	245	928	0.26
oc15c195	0.07469	0.00280	0.01184	0.00018	0.20055	0.04893	0.00077	73	3	76	1	76	2	1.05	0.31	112	743	0.15
oc15c196	0.07605	0.00222	0.01175	0.00018	0.25802	0.04794	0.00051	74	2	75	1	75	2	0.17	0.68	298	1473	0.20
oc15c197	0.07850	0.00400	0.01168	0.00028	0.23697	0.04996	0.00071	77	4	75	2	75	3	0.24	0.62	196	698	0.28
oc15c198	0.07819	0.00230	0.01206	0.00020	0.27975	0.04678	0.00059	76	2	77	1	77	2	0.14	0.71	174	672	0.26
oc15c204	0.07570	0.00276	0.01166	0.00021	0.24812	0.04701	0.00067	74	3	75	1	75	3	0.06	0.80	128	617	0.21
oc15c205	0.07576	0.00288	0.01181	0.00021	0.22938	0.04934	0.00066	74	3	76	1	76	3	0.32	0.57	108	613	0.18
oc15c206	0.07470	0.00437	0.01189	0.00032	0.23236	0.04819	0.00118	73	4	76	2	76	4	0.53	0.47	50	162	0.31
oc15c207	0.07513	0.00462	0.01186	0.00030	0.20810	0.04922	0.00084	74	4	76	2	76	4	0.32	0.57	75	557	0.14

continued on next page

Appendix 2. *continued*

	Measured isotopic ratios							Calculated ages										
Analysis	$^{207}Pb/^{235}U$	1σ err.	$^{206}Pb/^{238}U$	1σ err.	Rho	$^{207}Pb/^{206}Pb$	1σ err.	$^{207}Pb/^{235}U$ Ma	1σ err. Ma	$^{206}Pb/^{238}U$ Ma	1σ err. Ma	Conc. age (Ma)	2σ err. Ma	MSWD of conc.	Prob. of conc.	Th ppm	U ppm	Ratio Th/U
Road - FP Dyke																		
oc15B59	0.0748	0.0033	0.0114	0.0003	0.3057	0.0490	0.0006	73	3	73	2	73	4	0.00	0.97	195	1160	0.17
oc15B62	0.0787	0.0054	0.0121	0.0004	0.2268	0.0484	0.0008	77	5	78	2	78	5	0.02	0.88	156	1113	0.14
oc15B63	0.0766	0.0023	0.0115	0.0002	0.2708	0.0477	0.0005	75	2	74	1	74	2	0.34	0.56	295	1549	0.19
oc15B64	0.0766	0.0040	0.0115	0.0004	0.3214	0.0498	0.0006	75	4	74	2	74	5	0.07	0.79	121	973	0.12
oc15B65	0.0761	0.0028	0.0111	0.0003	0.3939	0.0494	0.0005	74	3	71	2	72	4	1.59	0.21	194	2772	0.07
oc15B66	0.0803	0.0027	0.0121	0.0003	0.3152	0.0494	0.0006	78	3	78	2	78	3	0.10	0.75	105	779	0.13
oc15B68	0.0751	0.0028	0.0116	0.0002	0.2182	0.0499	0.0007	74	3	74	1	74	2	0.09	0.76	154	1117	0.14
oc15B73	0.0771	0.0020	0.0117	0.0002	0.3286	0.0467	0.0005	75	2	75	1	75	2	0.03	0.85	318	1632	0.19
oc15B75	0.0762	0.0033	0.0114	0.0003	0.2799	0.0502	0.0007	75	3	73	2	73	3	0.18	0.67	177	1079	0.16
oc15B76	0.0772	0.0021	0.0115	0.0002	0.3091	0.0487	0.0005	76	2	74	1	74	2	0.98	0.32	284	1789	0.16
oc15B77	0.0769	0.0026	0.0117	0.0003	0.3673	0.0469	0.0006	75	2	75	2	75	3	0.03	0.86	78	1119	0.07
oc15B78	0.0753	0.0044	0.0118	0.0003	0.2512	0.0496	0.0009	74	4	76	2	76	4	0.26	0.61	46	526	0.09
oc15B80	0.0763	0.0027	0.0114	0.0002	0.2957	0.0494	0.0006	75	3	73	2	73	3	0.39	0.53	323	1680	0.19
oc15B81	0.0762	0.0030	0.0112	0.0003	0.3589	0.0496	0.0005	75	3	72	2	73	4	0.82	0.37	317	2246	0.14
oc15B82	0.0765	0.0028	0.0117	0.0003	0.3160	0.0486	0.0005	75	3	75	2	75	3	0.00	0.94	137	1411	0.10
oc15B83	0.0773	0.0029	0.0113	0.0003	0.3493	0.0496	0.0007	76	3	72	2	73	4	1.37	0.24	154	1106	0.14
oc15B84	0.0784	0.0038	0.0119	0.0003	0.2704	0.0484	0.0008	77	4	76	2	76	4	0.00	0.95	124	449	0.28
oc15B85	0.0767	0.0060	0.0118	0.0006	0.3005	0.0501	0.0007	75	6	76	4	75	7	0.01	0.93	183	491	0.37
oc15B86	0.0758	0.0051	0.0116	0.0004	0.2625	0.0499	0.0012	74	5	75	3	74	5	0.00	0.95	54	259	0.21
oc15B60	0.0847	0.0056	0.0132	0.0004	0.2448	0.0482	0.0006	83	5	85	3	84	5	0.16	0.69	298	1388	0.21
oc15B61	0.5102	0.0686	0.0679	0.0076	0.4148	0.0551	0.0009	419	46	423	46	421	77	0.01	0.92	90	170	0.53
oc15B69	0.0834	0.0300	0.0117	0.0011	0.1305	0.0561	0.0014	81	28	75	7	75	14	0.05	0.82	156	1311	0.12
oc15B74	0.0938	0.0083	0.0146	0.0006	0.2126	0.0539	0.0011	91	8	94	4	93	7	0.11	0.74	29	227	0.13
oc15B79	0.2904	0.0440	0.0414	0.0042	0.3370	0.0582	0.0008	259	35	262	26	261	48	0.01	0.94	166	212	0.78

Appendix 3. *LAM ICP-MS U-Pb analytical data for magmatic zircon from Amadeus stock.*

	Measured isotopic ratios							Calculated ages										
Analysis	$^{207}Pb/^{235}U$	1σ err.	$^{206}Pb/^{238}U$	1σ err.	Rho	$^{207}Pb/^{206}Pb$	1σ err.	$^{207}Pb/^{235}U$ Ma	1σ err. Ma	$^{206}Pb/^{238}U$ Ma	1σ err. Ma	Conc. age (Ma)	2σ err. Ma	MSWD of conc.	Prob. of conc.	Th ppm	U ppm	Ratio Th/U
oc15B21	0.07276	0.00448	0.01157	0.00045	0.31412	0.04766	0.00069	71	4	74	3	73	5	0.43	0.51	247	1247	0.20
oc15B23	0.07513	0.00454	0.01205	0.00034	0.23537	0.04730	0.00063	74	4	77	2	77	4	0.71	0.40	378	1130	0.33
oc15B24	0.07474	0.00345	0.01175	0.00040	0.37173	0.04713	0.00060	73	3	75	3	75	5	0.40	0.53	183	718	0.26
oc15B25	0.07445	0.00458	0.01184	0.00037	0.25223	0.04811	0.00077	73	4	76	2	75	4	0.46	0.50	181	761	0.24
oc15B26	0.07642	0.00811	0.01200	0.00052	0.20606	0.05105	0.00079	75	8	77	3	77	7	0.07	0.79	258	1022	0.25
oc15B27	0.08179	0.00510	0.01215	0.00062	0.40771	0.04946	0.00064	80	5	78	4	79	7	0.17	0.68	92	1272	0.07
oc15B28	0.07868	0.00373	0.01204	0.00037	0.32069	0.04744	0.00066	77	4	77	2	77	4	0.00	0.95	241	1093	0.22
oc15B29	0.07987	0.00324	0.01209	0.00036	0.36970	0.04698	0.00068	78	3	77	2	78	4	0.03	0.85	252	1050	0.24
oc15B30	0.07652	0.00350	0.01197	0.00032	0.29629	0.04774	0.00055	75	3	77	2	76	4	0.30	0.58	233	1156	0.20
oc15B31	0.07441	0.00309	0.01184	0.00026	0.26163	0.04802	0.00052	73	3	76	2	75	3	1.05	0.31	436	1520	0.29
oc15B36	0.07620	0.00265	0.01157	0.00022	0.27629	0.04983	0.00064	75	3	74	1	74	3	0.03	0.87	518	1326	0.39
oc15B37	0.07920	0.00459	0.01194	0.00032	0.23172	0.04958	0.00086	77	4	76	2	77	4	0.04	0.84	163	736	0.22
oc15B38	0.07997	0.00326	0.01199	0.00027	0.27264	0.04873	0.00080	78	3	77	2	77	3	0.18	0.67	302	922	0.33
oc15B39	0.07613	0.00290	0.01177	0.00030	0.33385	0.04805	0.00059	75	3	75	2	75	4	0.11	0.74	472	1236	0.38
oc15B40	0.08051	0.00341	0.01178	0.00036	0.36148	0.04924	0.00067	79	3	75	2	76	4	0.97	0.33	193	829	0.23
oc15B41	0.07515	0.00351	0.01137	0.00035	0.33211	0.04834	0.00068	74	3	73	2	73	4	0.04	0.84	194	1061	0.18
oc15B42	0.07925	0.00442	0.01166	0.00037	0.28732	0.04939	0.00082	77	4	75	2	75	5	0.42	0.52	270	1133	0.24
oc15B43	0.07540	0.00341	0.01179	0.00031	0.28655	0.04758	0.00064	74	3	76	2	75	4	0.29	0.59	234	1179	0.20
oc15B44	0.07763	0.00535	0.01203	0.00044	0.26259	0.04848	0.00074	76	5	77	3	77	5	0.05	0.82	347	868	0.40
oc15B46	0.07622	0.00257	0.01130	0.00025	0.33352	0.04876	0.00058	75	2	72	2	73	3	0.78	0.38	330	1542	0.21
oc15B50	0.07914	0.00578	0.01187	0.00038	0.21988	0.04997	0.00083	77	5	76	2	76	5	0.05	0.82	291	986	0.30
oc15B51	0.07758	0.00526	0.01179	0.00043	0.26690	0.05000	0.00079	76	5	76	3	76	5	0.00	0.95	179	765	0.23
oc15B53	0.07283	0.00390	0.01209	0.00029	0.22094	0.04539	0.00075	71	4	77	2	77	4	2.68	0.10	345	899	0.38
oc15B54	0.07238	0.00588	0.01191	0.00052	0.26988	0.04644	0.00067	71	6	76	3	75	6	0.90	0.34	349	1091	0.32
oc15B55	0.07437	0.00232	0.01180	0.00020	0.27170	0.04677	0.00058	73	2	76	1	75	2	1.57	0.21	233	1386	0.17
oc15B20	0.08081	0.00311	0.01101	0.00022	0.26420	0.05685	0.00056	79	3	71	1	71	3	8.25	0.00	796	2608	0.31
oc15B22	0.06773	0.00790	0.01184	0.00024	0.08599	0.06018	0.00141	67	8	76	2	76	3	1.55	0.21	289	1045	0.28